2018 26th Mediterranean Conference on Control and Automation (MED)
Zadar, Croatia, June 19-22, 2018

Localization of an Array of Hydrophones Towed by an Autonomous Underwater Vehicle

Filippo Arrichiello, Soumic Sarkar, Stefano Chiaverini, Gianluca Antonelli

Abstract— **The paper addresses the localization problem of an array of hydrophones mounted on a flexible streamer towed by an Autonomous Underwater Vehicle (AUV). The considered system has been developed in the framework of the H2020 European project WiMUST and it is finally aimed at performing seismic surveys by acoustic means to explore the sea bottom subsurface. In particular, in the project's scenario, the acoustic seismic survey is performed having two autonomous surface vessels, carrying acoustic sources named sparkers, and a team of AUVs, towing a streamer each. The time of flight with which the waves generated from the sparkers reflect in the sea sub-bottom layers and return to the hydrophones provides valuable information about the properties of the ocean subsurface. However, for a proper processing of the acoustic data, there is the need to estimate the hydrophones' positioning. Here, we present a localization strategy for the described system based on an Extended Kalman Filter (EKF) that uses the dynamic model of the AUV-streamer system and the range measurements from sparkers to hydrophones as extracted from the seismic acoustic signals. The proposed approach has been tested in numerical case studies built using data extracted from the experimental tests performed in the framework of the WiMUST project.**

I. Introduction

With the advent of robotics research to facilitate navigation in hazardous environments, Autonomous Underwater Vehicles (AUVs) find their applications both for scientific and commercial purposes. A wide overview on design, modelling, navigation and control of such vehicles can be found in [1], [2]. Here, the prime focus is to explore issues related to the use of AUVs for seismic acoustic surveys, with the purpose of exploring sea bottom subsurfaces to cater to the applications like oil and gas exploration, and civil and commercial underwater constructions. Traditionally, the seismic acoustic survey is performed using a surface vessel carrying powerful acoustic sources, known as sparkers, and towing a set of streamers equipped with several hydrophones to record acoustic signals. The sparkers generate seismic waves by intermittently releasing electric pulses that produce low frequency sound waves. Such waves travel towards the sea floor and are reflected back to the hydrophones on the streamers. The time of flight with which waves return to the surface, registered with the hydrophones, provides valuable information regarding the properties of the ocean subsurface. The acoustic data gathered with the hydrophones can then be processed with different techniques [3]. As an example, the use of Matched-Field Processing (MFP) for geoacoustic parameters estimation was presented in [4], and then extended to a variety of setups like fixed vertical arrays [5], towed arrays [6], drifting arrays using surface noise [7], and with vector sensor recently [8].

Authors are with the Department of Electrical and Information Engineering of the University of Cassino and Southern Lazio, Via G. Di Biasio 43, 03043 Cassino (FR), Italy {f.arrichiello, chiaverini, antonelli}@unicas.it, soumic4it@gmail.com

Fig. 1. Sketch of the WiMUST multi-robot system.

The H2020 European Project named Widely scalable Mobile Underwater Sonar Technology (WiMUST) [9] aimed at enabling distributed acoustic array technologies for seismic surveying by mean of cooperative marine robotic systems. The main goal of the project was to develop a robotic system capable to perform seismic survey missions in which autonomous surface vessels carry the sparkers, and a team of AUVs, towing a streamer of hydrophones each, navigates in formation to properly acquire the acoustic signals. Such system presents several advantages as the possibility to change the positions of the AUVs to modify the geometry of the 3D acoustic array of hydrophones and to improve the quality of the sea bottom exploration. Moreover, the possibility to move the AUVs close to the seabed can allow more in depth analysis of the sea subsurface, or to reduce the power of the acoustic signal generators. On the other side, the development of a team of AUVs that has to cooperate despite the low-bandwidth of the acoustic communication link, and the need to operate in scenario in which localization infrastructure are unavailable, make the project particularly challenging from both theoretical and technological issues.

For a proper processing of the acoustic data, there is the need to know the hydrophones' positioning; however, the absence of a localization infrastructure requires the development of a strategy to estimate the hydrophones' positioning from the available set of information. To the purpose, in this paper we present a localization strategy for the AUV-streamer system that, beyond using the data from navigation sensor of the AUV, as gyroscope, compass, Inertial Measurement Unit (IMU), Ultra-Short Base Line (USBL) (as in [10]), it also makes use of information gathered from acoustic signals generated for the seismic survey. Indeed, considering that the

978-1-5386-7891-6/18/$31.00 ©2018 IEEE

sparkers and AUVs can be equipped with acoustic modems with atomic clocks that allow precise synchronization, it is possible to use the direct time of arrival of the acoustic signals from the sparker to the hydrophones to compute range measurements. Thus, in the proposed localization strategy, range measurements from sparker to each hydrophone are collected and fused with AUV on board navigation sensors to estimate the overall system state using an Extended Kalman Filter (EKF). In the considered case, the streamer is a long and almost neutrally buoyant flexible cable equipped with a set of hydrophones. For the EKF prediction step we derive the dynamic model of the AUV-streamer system considering the AUV as a fully-actuated rigid body, and the streamer as a serial chain of rigid links with a spherical unactuated joint in correspondence of each hydrophone [11], [12]. The underwater dynamics of each rigid body has been modelled following the approach in [13]. In particular, the parameters of the dynamic model of the AUV have been defined on the basis of the Folaga Vehicles characteristics, i.e. a $2m$-length torpedo shaped AUV, used for the WiMUST project purposes; the streamer, instead, has been modeled as a set of almost neutrally buoyant thin cylindrical elements connected via unactuated spherical joints. Hydrodynamic terms and drag coefficients have been chosen accordingly to the effective geometry of the system, and on the basis of the common velocity regimes of the WiMUST system (i.e. cruise velocity about $1\,m/s$). Given the large dimension of the overall system state, the direct dynamic function, needed for both numerical simulations of the system dynamics and for the computation of the prediction terms of the EKF, has been developed referring to the Newton-Euler recursive procedure used for industrial manipulators [14].

The overall localization strategy has been extensively tested in numerical simulations in Matlab environment, considering the case of single and multiple sparkers, and considering the AUV equipped with different set of navigation sensors. Moreover, the localization algorithm has been tested using data gathered from the experimental tests performed in Sines, Portugal (Nov. 2016) for the WiMUST project purposes. A preliminary study on the feasibility of the localization strategy of the AUV-streamer system considering the availability of range measurements from the sparkers has been investigated in [15]; however, that study was based on the use of an instantaneous set of sensor data, thus assuming the system as static. In this paper we extend such work by considering the AUV-streamer dynamic model presented in [16] for the derivation of the equations of an EKF; then, we performed numerical validations by simulating the motion of an AUV following specific trajectories (i.e. no more based on a single set of sensor data from an instantaneous configuration), and by integrating data from experimental tests in the numerical validation.

II. Dynamic Modelling of AUV-Streamer System

In this section, we summarise the main equations for the AUV-streamer dynamic model, while the step-by-step derivations of these equations can be found in [16].

Notations: In this paper, any frame $\{k\}$ in small letter has the origin at a point K in capital letter; any vector $\mathbf{r}_A^b$ denotes a vector from the origin of the inertial frame to the point A expressed in a frame $\{b\}$; any vector $\mathbf{r}_{AB}^c$ denotes a position vector from a point A to another point B expressed in a frame $\{c\}$; any vector $\mathbf{v}_A^b$ denotes the velocity of the point A with respect to the frame $\{i\}$ expressed in $\{b\}$; any vector $\boldsymbol{\omega}_{ab}^c$ denotes the angular velocity of a frame $\{b\}$ with respect to another frame $\{a\}$ expressed in a frame $\{c\}$; any matrix $\mathbf{R}_a^b$ denotes a rotation matrix of a frame $\{a\}$ with respect to another frame $\{b\}$; any vector $\boldsymbol{\eta}_a^b$ denotes the vector of the Euler angles of frame $\{a\}$ with respect to another frame $\{b\}$; any matrix $\mathbf{T}_{\boldsymbol{\eta}_a^b}$ denotes the angular transformation that transforms the angular velocity to Euler rate, the vector $\boldsymbol{\eta}_a^b$ being the vector of Euler angles; any vector $\mathbf{T}_i$ denotes the tension force applied by the link $i+1$ on the link i; any vector $\mathbf{f}_j^i$ denotes a force expressed in the frame $\{i\}$; any vector $\boldsymbol{\tau}_j^i$ denotes a torque expressed in the frame $\{i\}$.

Referring to Fig. 2, we assume that the AUV is a rigid body with centroid in C; the streamer is attached to the AUV's hull in the point P, and the $i-th$ hydrophone position is denoted as P_i. The streamer, that is a long, flexible and neutrally buoyant cable, is modeled as a serial chain of rigid links with a spherical unactuated joint in P and one in correspondence of each hydrophone P_i. In particular, the equations of each element are derived considering inertia, drag, buoyancy, external forces and force exchanged with the connected elements.

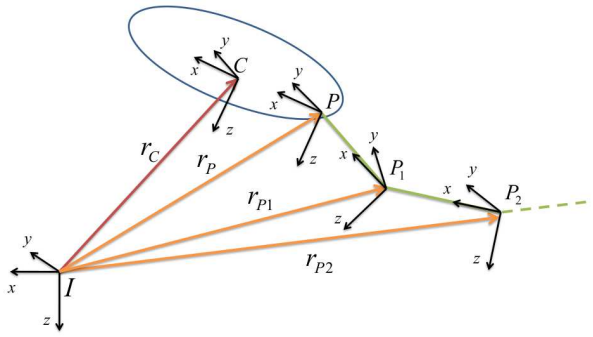

Fig. 2. Sketch of an AUV towing a streamer of hydrophones.

Newton-Euler equations of the AUV:
The Newton-Euler equations for the AUV can be expressed as

$$
\begin{aligned}
&m_{auv}\left(\dot{\mathbf{v}}_P^i + S(\dot{\boldsymbol{\omega}}_{ic}^i)\mathbf{r}_{PC}^i + S^2(\boldsymbol{\omega}_{ic}^i)\mathbf{r}_{PC}^i\right) = \mathbf{f}_{auv}\\
&m_{auv}S(\mathbf{r}_{PC}^i)\dot{\mathbf{v}}_P^i + \mathbf{I}_P^i\dot{\boldsymbol{\omega}}_{ip}^i + S(\boldsymbol{\omega}_{ip}^i)\mathbf{I}_P^i\boldsymbol{\omega}_{ip}^i = \boldsymbol{\tau}_P^i\\
&\mathbf{f}_{auv} = \mathbf{f}_{act} + \mathbf{f}_{drag} + \mathbf{f}_b + \mathbf{f}_g + \mathbf{T}_0\\
&\boldsymbol{\tau}_P^i = \boldsymbol{\tau}_{act}^i + \boldsymbol{\tau}_{drag}^i + \boldsymbol{\tau}_0^i + \mathbf{r}_{PC}^i \times \mathbf{f}_{act} + \mathbf{r}_{PC}^i \times \mathbf{f}_g\\
&+ \mathbf{r}_{PB}^i \times \mathbf{f}_b
\end{aligned}
$$

where m_{auv} is the AUV mass, $S(\boldsymbol{\omega})$ is the skew-symmetric matrix having for elements those of the angular velocity vector $\boldsymbol{\omega}$, $\mathbf{f}_{auv}$ is the sum of the forces acting on the AUV (respectively $\mathbf{f}_{act}$, $\mathbf{f}_{drag}$, $\mathbf{f}_b$, and $\mathbf{f}_g$ are the actuation, drag,

buoyancy, gravity forces and $\mathbf{T}_0$ is the force applied by the streamer), $\mathbf{I}^i_P$ is the Inertia Matrix computed with pole in P, τ_{auv} is the sum of the torques acting on the AUV (τ_{act}, τ_{drag}, are the actuation, drag torques).

Newton-Euler equations of the $i^{th}-$ link:
The Newton-Euler equations for the $i^{th}-$ link can be expressed as

$$\begin{aligned}
&m_i(\dot{\mathbf{v}}^i_{P_i} + S(\dot{\boldsymbol{\omega}}^i_{ip_i})\mathbf{r}^i_{P_iC_i} + S^2(\boldsymbol{\omega}^i_{ip_i})\mathbf{r}^i_{P_iC_i}) = \mathbf{f}^i_i \\
&m_i S(\mathbf{r}^i_{P_iC_i})\dot{\mathbf{v}}^i_{P_i} + \mathbf{I}^i_{P_i}\dot{\boldsymbol{\omega}}^i_{ip_i} + S(\boldsymbol{\omega}^i_{ip_i})\mathbf{I}^i_{P_i}\boldsymbol{\omega}^i_{ip_i} = \boldsymbol{\tau}^i_{P_i} \\
&\mathbf{f}^i_i = \mathbf{f}_{dragi} + \mathbf{f}_{bi} + \mathbf{f}_{gi} + \mathbf{T}_i - \mathbf{T}_{i-1} \\
&\boldsymbol{\tau}^i_{P_i} = -\boldsymbol{\tau}^i_{i-1} + \boldsymbol{\tau}^i_i + \boldsymbol{\tau}^i_{dragi} + \mathbf{r}^i_{P_iB_i} \times \mathbf{f}_{bi} \\
&+ \mathbf{r}^i_{P_iP_{i-1}} \times (-\mathbf{T}_{i-1}) + \mathbf{r}^i_{P_iC_i} \times \mathbf{f}_{gi} + \mathbf{r}^i_{P_iC_i} \times \mathbf{f}_{dragi}
\end{aligned}$$

For both numerical simulation purposes and for the derivation of the EKF prediction equations, the dynamic model of the system must be rewritten in a state space form. Thus, let us denote $\mathbf{q} = [\mathbf{r}^i_C, \boldsymbol{\eta}^i_c, \boldsymbol{\eta}^{p_n}_p]^T$, where $\boldsymbol{\eta}^{p_n}_p = [\boldsymbol{\eta}^{p_1}_p, \boldsymbol{\eta}^{p_2}_{p_1}, ..., \boldsymbol{\eta}^{p_n}_{p_{n-1}}]$, and $\boldsymbol{\tau} = [\mathbf{f}^i_c, \boldsymbol{\tau}^i_c, \boldsymbol{\tau}^i_{P_i}]^T$ where $\boldsymbol{\tau}^i_{P_i} = [\boldsymbol{\tau}^i_{P_1}, ..., \boldsymbol{\tau}^i_{P_n}]$. The dynamic model can be rewritten as:

$$\begin{aligned}
\ddot{\mathbf{q}} &= \mathbf{M}(\mathbf{q})^{-1}(\boldsymbol{\tau} - \overline{\boldsymbol{\tau}}) \\
\overline{\boldsymbol{\tau}} &= \mathbf{C}(\mathbf{q}, \dot{\mathbf{q}})\dot{\mathbf{q}} + \mathbf{F}_{drag}(\dot{\mathbf{q}}) + \mathbf{F}_b(\mathbf{q}) + \mathbf{F}_g(\mathbf{q})
\end{aligned} \tag{1}$$

where $\mathbf{M}$ is the mass matrix; $\boldsymbol{\tau}$ is the actuation forces and torques; $\mathbf{C}(\mathbf{q}, \dot{\mathbf{q}})$ is the centrifugal and coriolis matrix; $\mathbf{F}_{drag}$ is the drag forces and torques; $\mathbf{F}_b$ is buoyancy forces and torques; $\mathbf{F}_g$ is the gravitational forces and torques. Then, defining the state variable $\mathbf{x} = [\mathbf{q}, \dot{\mathbf{q}}]^T$, from eq.(1) the model can be reformulated in the form $\dot{\mathbf{x}} = \mathbf{f}(\mathbf{x}, \mathbf{u})$, where the $\mathbf{u}$ is the input term.

Since the number of hydrophones can be of the order of tens, the dimensions of the system state vector can be very large; thus the equations in (1) can not be easily computed in a closed form. Thus, we refer to the Newton-Euler recursive algorithm for industrial manipulators [14] to numerically compute on-line the direct dynamic function.

III. AUV-STREAMER LOCALIZATION ALGORITHM

To develop the AUV-streamer localization algorithm, we refer to a discrete time version of the Extended Kalman Filter. Thus, we started by discretizing the continuous time dynamic model:

$$\mathbf{x}_k = f(\mathbf{x}_{k-1}, \mathbf{u}_{k-1}) + \mathbf{w}_{k-1} \tag{2}$$

where $\mathbf{x}_k = [q_k, \dot{q}_k]^T \in \mathbb{R}^{2(6+3no\_of\_links)}$ and $f(\mathbf{x}_{k-1}, \mathbf{u}_{k-1})$ is the state transition function.

A. Sensors

Then, we defined the output measurements function as

$$\boldsymbol{\alpha}_k = h(\mathbf{x}_k) + \mathbf{v}_k \tag{3}$$

$\boldsymbol{\alpha_k}$ represents the set of output measurements available to the system, $h(\mathbf{x}_k)$ and $\mathbf{v}_k$ are the output function and noise respectively. To build the output function, we assume that the AUV is equipped with various proprioceptive and relative localization sensors, which can be employed depending on specific operational mode. We define below the relative equations and we assume that all the measurements are affected by zero-mean gaussian noise. Their formulation will be then used in the development of the EKF output function, and in the computation of the Jacobian matrix used in the covariance correction equation. The considered sensors are:

- *Compass:* that gives the actual yaw information of the AUV as described by the following equation

$$\alpha_{comp} = \psi_k + v_{comp} \tag{4}$$

where $v_{comp} \sim \mathcal{N}(0, \sigma^2_{comp})$ is the noise term.
- *Ultra-short Baseline (USBL):* that is an acoustic positioning system for the underwater vehicle navigation and tracking. The measurement equation of this sensor is given as follows

$$\alpha_{usbl} = [x_k \ y_k \ z_k]^T + \mathbf{v}_{usbl} \tag{5}$$

where $\mathbf{v}_{usbl} \sim \mathcal{N}(0, \sigma^2_{usbl})$ is the noise term.
- *Depth Sensor:* that gives the actual depth information of the AUV from the sea surface as described by the following equation

$$\alpha_{depth} = z_k + v_{depth} \tag{6}$$

where $v_{depth} \sim \mathcal{N}(0, \sigma^2_{depth})$ is the noise term.
- *Gyroscope:* that is used to measure the orientation with respect to the inertial frame of the body to which the sensor is attached to. Generally, the Euler angles, roll, pitch, and yaw are measured using this sensor, and the relative equation is given as

$$\alpha_{gyro} = [\phi_k \ \theta_k \ \psi_k]^T + \mathbf{v}_{gyro} \tag{7}$$

where $v_{gyro} \sim \mathcal{N}(0, \sigma^2_{gyro})$ is the noise term.
- *Doppler Velocity Log (DVL)/IMU*: that is the couple of sensors that allow to measure linear and angular velocity. In a discrete time formulation, its output, including the effect of the sample time dT, is given by

$$\alpha_{dvl} = \begin{bmatrix} x_k - x_{k-1} \\ y_k - y_{k-1} \\ z_k - z_{k-1} \\ \theta_k - \theta_{k-1} \\ \psi_k - \psi_{k-1} \end{bmatrix} + \mathbf{v}_{dvl} \tag{8}$$

where $\mathbf{v}_{dvl} \sim \mathcal{N}(0, R_{v,dvl})$ is the noise term.
- *Range from Sparkers:* we assume that the AUV can directly collect information from the hydrophones on the streamer and, from the time of flight of acoustic signals, it can compute the range measurements from each hydrophone X_{P_i} and to a sparker in position $X_S = [x_S, y_S, z_S]^T$. The output equation is:

$$\alpha_{range} = \parallel X_{P_i} - X_R \parallel + v_{range} \tag{9}$$

where $v_{range} \sim \mathcal{N}(0, \sigma^2_{range})$ is noise term.

B. Discrete-time EKF prediction and update equations

As is well known, the Extended Kalman Filter is a two steps process. In the first step, a prediction of state and covariance is computed on the base of the state space dynamic model and on the system input. In the second step, a correction is performed on the base of the available sensor models and readings. The set of equations is reported below:

- **State and covariance prediction**

$$\widehat{\mathbf{x}}_{k|k-1} = f(\widehat{\mathbf{x}}_{k-1|k-1}, \mathbf{u}_{k-1}) \quad (10)$$

$$\mathbf{P}_{k|k-1} = \mathbf{F}_{k-1}\mathbf{P}_{k-1|k-1}\mathbf{F}_{k-1}^T + \mathbf{Q}_{k-1} \quad (11)$$

- **State and covariance update**

$$\boldsymbol{\beta}_k = \boldsymbol{\alpha}_k - h(\widehat{\mathbf{x}}_{k|k-1}) \quad (12)$$

$$\mathbf{S}_k = \mathbf{H}_k\mathbf{P}_{k|k-1}\mathbf{H}_k^T + \mathbf{R}_k \quad (13)$$

$$\mathbf{K}_k = \mathbf{P}_{k|k-1}\mathbf{H}_k^T\mathbf{S}_k^{-1} \quad (14)$$

$$\widehat{\mathbf{x}}_{k|k} = \widehat{\mathbf{x}}_{k|k-1} + \mathbf{K}_k\boldsymbol{\beta}_k \quad (15)$$

$$\mathbf{P}_{k|k} = (\mathbf{I} - \mathbf{K}_k\mathbf{H}_k)\mathbf{P}_{k|k-1} \quad (16)$$

where the Jacobians of the state transition and observation functions $f(\mathbf{x}_{k-1}, \mathbf{u}_{k-1})$ and $h(\mathbf{x}_k)$ are calculated respectively around the small neighbourhood δ and ϵ of the points $\widehat{\mathbf{x}}_{k-1|k-1}, \mathbf{u}_{k-1}$ and $\widehat{\mathbf{x}}_{k|k-1}$ respectively as given by the following equations:
$\mathbf{F}_{k-1} = \frac{\partial f}{\partial \boldsymbol{x}}\Big|_{\hat{\boldsymbol{x}}_{k-1|k-1}, \boldsymbol{u}_{k-1}}$ and $\boldsymbol{H}_k = \frac{\partial h}{\partial \boldsymbol{x}}\Big|_{\hat{\boldsymbol{x}}_{k|k-1}}$.

IV. Numerical validation

To validate the approach we develop in Matlab environment all the equations described in the previous section. In particular, we firstly derived the inverse and direct dynamic function of the AUV-streamer system following the procedure described in III. The values of the parameters of the dynamic models of the AUV and of the streamer have been chosen on the base of the geometry of one of the class of AUVs used in the WiMUST project, i.e. the Folaga AUVs, and on the base of the geometric characteristics of the streamer developed for the project purposes, see Fig. 3. The values of the main parameters are reported in the following table:

AUV parameters	
Folaga Length	$2\ m$
Folaga Diameter	$0.155\ m$
Centroid to point of attachment	$1\ m$
Link Parameters	
Link Length	$1.0\ m$
Link Diameter	$0.035\ m$
Environment Parameters	
Water Density	$1.02\ m$
Gravitational Acceleration	$9.81\ m$

The standard deviation of the noise term of the sensors described in Section III have been chosen as:

Fig. 3. Snapshot of a team of AUVs equipped with streamer of hydrophones.

EKF parameters	
$\sigma_{usbl} = 0.2\ m$	$\sigma_{depth} = 0.1\ m$
$\sigma_{gyro} = (2/180)\pi\ rad$	$\sigma_{range} = 0.1\ m$
DVL (linear velocity)	$\sigma_{dvl,x} = 0.1\ m$ $\sigma_{dvl,y} = 0.1\ m$ $\sigma_{dvl,z} = 0.1\ m$
DVL (Euler rate)	$\sigma_{dvl,\phi} = 2^\circ$ $\sigma_{dvl,\theta} = 2^\circ$ $\sigma_{dvl,\psi} = 2^\circ$

Fig. 4 shows a snapshot of a graphical representation of the system that we used to compare the actual and the estimated positions of the AUV and of the hydrophones position in the numerical simulation. The green ellipse represents the AUV, and the series of encircled points, attached to its tail-like streamer, are the positions of the eight hydrophones. The dynamic simulations have been run in MATLAB assuming a sample time of $0.1s$.

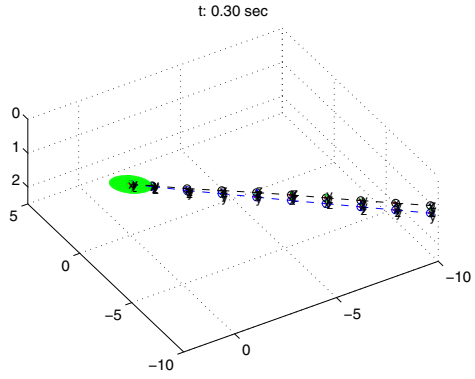

Fig. 4. Snapshot of actual and estimated positions of AUV and hydrophones in the graphical animation.

For validation purposes we tested the algorithm both via pure numerical simulations, considering different sets of available sensors and one or multiple sparkers, and in simulations generated using a set of data taken from real experimental tests performed in the water. For lack of space, we report here the sole simulation case study developed using the experimental data. To the purpose, we used the data collected during an experimental campaign performed in the framework of the first integration week of the WiMUST project, held in Sines, Portugal, on November 2016. The collected data refer to a set of experiments performed with an AUV navigating at the sea surface (so that GPS measurements were available and stored) in a harbor area. The AUV towed a ten meter streamer equipped with eight hydrophones, at the distance of 1 m one from the other. A sparker mounted on a moored buoy was firing acoustic signals at a frequency of $1Hz$. Both the AUV and the sparker were equipped with Evologic acoustic modems with atomic clocks; thus, the acoustic signal generator (on the sparker) and the acoustic receivers (the hydrophones) were accurately time synchronized. The acoustic signals collected with the hydrophones were stored in the format of SEG-Y files, i.e. the standard format for storing geophysical data. Specifically, the SEG-Y file contains a set of traces for each hydrophone, where a trace represents the progress of the acoustic signal in a time slot of predefined length and time synchronized with the acoustic source. By post processing the SEG-Y file, beyond studying the sea subsurface from the signal reflections, it is also possible to extract the range measurement from the sparker to hydrophones by computing the direct time of arrival of the acoustic signal (i.e. the time to reach the hydrophone without reflection on the sea bottom). Figure 5 shows an example of the range data extracted from the SEG-Y file and filtered out of a set of outliers following a threshold base approach. Such data have been used in the following case study, together with the AUV's GPS measurements, to perform a realistic simulations of the localization approach performance. The GPS readings of the experiment with the AUV have been used as desired trajectory for a simulated AUV, where a basic PI controller has been used as a low-level dynamic control law.

In the EKF implementation, while the prediction equation runs at the frequency of $10Hz$, the correction part is built considering that the AUV sensors can have different frequency (e.g. USBL has a lower frequency than the gyro and the IMU), and range measurements from experimental data are used only when effectively available (approximately at the frequency of $1Hz$). Fig. 6 shows the actual and the estimated position of the AUV and of the hydrophones, while the AUV followed the desired path and the range measurements from the sparker were used. Fig. 7 shows the errors in the AUV position and velocity estimation, while Fig. 8 shows the errors of Euler angles and angles rates of the AUV estimation. The norm of the positioning estimation error for each hydrophone is plotted in Fig. 9. From the figure it can be noticed that, as can be expected, the estimation error decreases from the large initial error value, it keeps

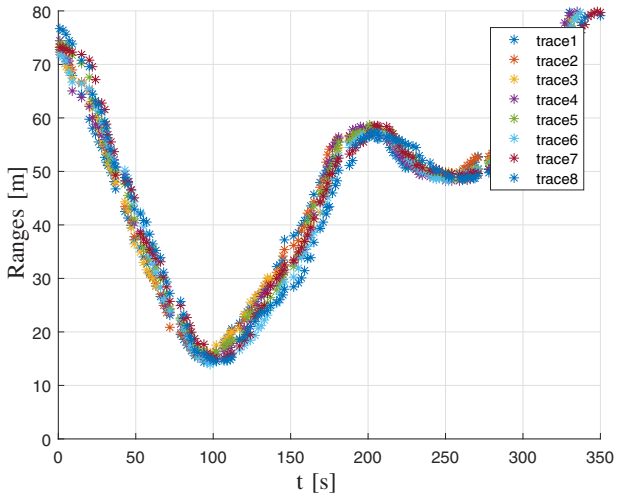

Fig. 5. Range measurements from the sparker to the hydrophones collected from seismic acoustic data.

relatively low values with oscillations due to the process and measurement noise, and it keeps highest values for the farthest hydrophone from the AUV.

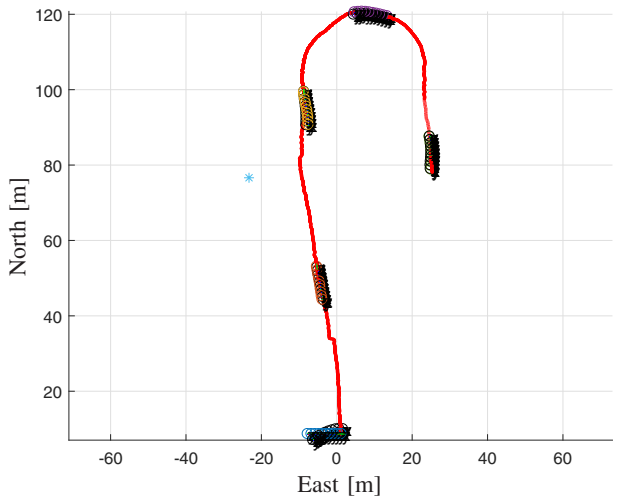

Fig. 6. Plot of the desired trajectory (red), and few snapshots showing the AUV and hydrophones real and estimated positions. The cyan star represents the position of the sparker.

V. Conclusion

This paper presents an EKF based localization strategy for an AUV towing a streamer with hydrophone. The dynamic model of the system has been derived simulating the behavior of the flexible streamer as an unactuated chain of rigid elements connected with spherical joints. Direct dynamic function were derived referring to recursive Newton-Euler approach for robotic manipulator. The approach has been validated via numerical simulations that make use of data from experimental tests in the water with an AUV towing a streamer, whose hydrophones recorded the acoustic signals generated from a sparker. The numerical validation shows the effectiveness of the proposed solution. Future works

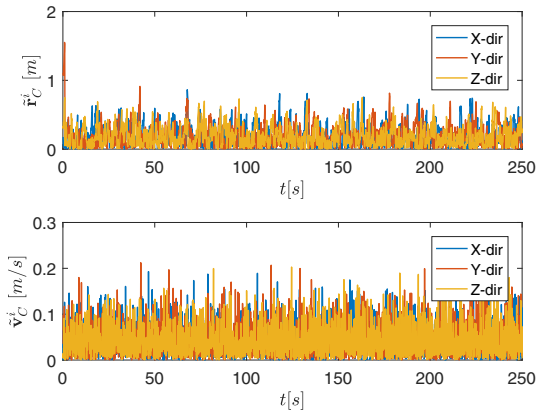

Fig. 7. Plot of the estimation error of AUV position and linear velocity.

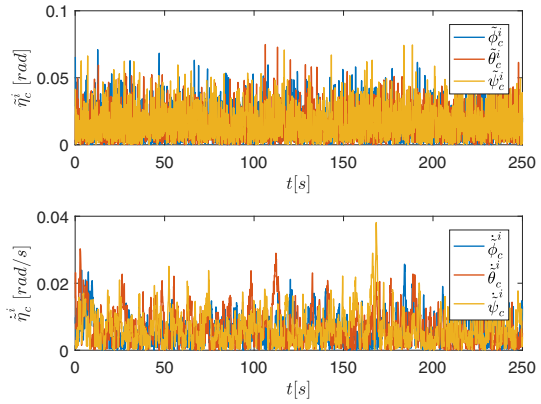

Fig. 8. Plot of the estimation error of AUV Euler Angles and Euler rates.

are aimed at integrating the developed algorithm in the navigation algorithm of the AUV to be tested on line. Moreover, a limit of the proposed validation is related to the absence of a ground truth system to compute the real position of the hydrophones when underwater; a possibility to solve this issue is to equip the tail of the hydrophone with a further acoustic modem with USBL localization capabilities. Finally, we will extend the strategy to the case of a moving source, i.e. the case the sparker is towed by an autonomous vessel, and we will evaluate the effects of the presence of multiple sparkers as expected to be present in the final project results.

ACKNOWLEDGMENT

This work has received funding from the European Union's Horizon 2020 research and innovation programme under the grant agreement No. 645141 (WiMUST project). The Authors want to thank Henrique Duarte from Geosurvey for providing range measurements from seismic data, and the colleagues for IST of Lisbon for providing the AUV's experimental data.

REFERENCES

[1] T. Fossen, *Guidance and control of ocean vehicles*. Wiley, 1994.
[2] G. Antonelli, *Underwater Robots*, ser. Springer Tracts in Advanced Robotics. Springer International Publishing, 2013.

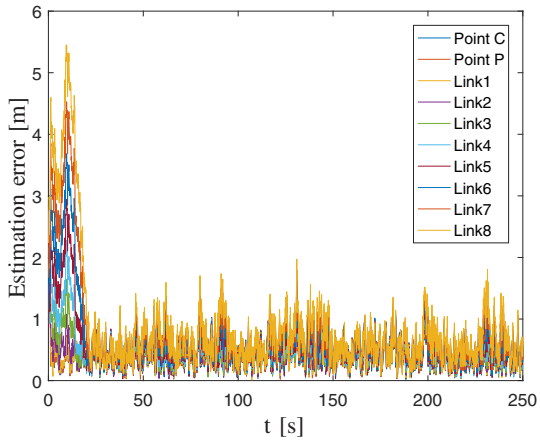

Fig. 9. Plot of the norms of the positions errors of the hydrophones.

[3] F. Barclay, A. Bruun, K. B. Rasmussen, J. C. Alfaro, A. Cooke, D. Cooke, D. Salter, R. Godfrey, D. Lowden, S. McHugo *et al.*, "Seismic inversion: Reading between the lines," *Oilfield Review*, vol. 20, no. 1, pp. 42–63, 2008.
[4] M. D. Collins, W. A. Kuperman, and H. Schmidt, "Nonlinear inversion for ocean-bottom properties," *The Journal of the Acoustical Society of America*, vol. 92, no. 5, pp. 2770–2783, 1992.
[5] M. Siderius, P. L. Nielsen, J. Sellschopp, M. Snellen, and D. Simons, "Experimental study of geo-acoustic inversion uncertainty due to ocean sound-speed fluctuations," *The Journal of the Acoustical Society of America*, vol. 110, no. 2, pp. 769–781, 2001.
[6] S. Jesus and A. Caiti, "Estimating geoacustic bottom properties from towed array data," *Journal of Computational Acoustics*, vol. 04, no. 03, pp. 273–290, 1996.
[7] C. H. Harrison, "Geoacoustic inversion of ambient noise," *The Journal of the Acoustical Society of America*, vol. 112, no. 5, pp. 2282–2282, 2002.
[8] P. Santos, O. Rodriguez, P. Felisberto, and S. Jesus, "Seabed geoacoustic characterization with a vector sensor array a," *The Journal of the Acoustical Society of America*, vol. 128, no. 5, pp. 2652–2663, 2010.
[9] P. Abreu, G. Antonelli, F. Arrichiello, A. Caffaz, A. Caiti, G. Casalino, N. C. Volpi, I. de Jong, D. D. Palma, H. Duarte *et al.*, "Widely scalable mobile underwater sonar technology: An overview of the h2020 wimust project," *Marine Technology Society Journal*, vol. 50, no. 4, pp. 42–53, 2016.
[10] F. Arrichiello, H. K. Heidarsson, and G. S. Sukhatme, "Opportunistic localization of underwater robots using drifters and boats," in *2012 IEEE International Conference on Robotics and Automation*, May 2012, pp. 5307–5314.
[11] J. E. Cochran, M. Innocenti, T. S. No, and A. Thukral, "Dynamics and control of maneuverable towed flight vehicles," *Journal of Guidance, Control, and Dynamics*, vol. 15, no. 5, pp. 1245–1252, Sep 1992.
[12] H. Hahn, *Rigid Body Dynamics of Mechanisms: 1 Theoretical Basis*. Springer Publishing Company, Incorporated, 2014.
[13] T. Fossen, *Marine Control Systems: Guidance, Navigation and Control of Ships, Rigs and Underwater Vehicles*. Trondheim, Norway: Marine Cybernetics, 2002.
[14] B. Siciliano, L. Sciavicco, L. Villani, and G. Oriolo, *Robotics: Modelling, Planning and Control*. Springer, 2009.
[15] F. Arrichiello, G. Antonelli, and E. Kelholt, "Shape estimate of a streamer of hydrophones towed by an autonomous underwater vehicle," *IFAC-PapersOnLine*, vol. 49, no. 23, pp. 181 – 186, 2016.
[16] S. C. F. Arrichiello, S. Sarkar and G. Antonelli, "Dynamic modelling of a streamer of hydrophones towed with an autonomous underwater vehicle," in *Modelling and Simulation for Autonomous Systems*, ser. Lecture Notes in Computer Science (LNCS, volume 10756), 2018, pp. 179–192.